X80管线钢埋弧焊接头性能分析

张 敏[1], 姚成武[1], 聂斌英[2]
(1.西安理工大学 材料科学与工程学院, 西安 710048;
2.宜春学院 工学院, 江西 宜春 336000)

张 敏

摘 要: 从焊接性和焊接接头使用性能两个方面入手, 结合焊接接头的硬度、拉伸和冲击韧度的测试, 对 X80管线钢的焊接性能进行了试验分析。结果表明, 焊接热影响区的性能发生了较大变化, 其中粗晶区出现硬化脆化现象, 并导致韧度下降, 而不完全重结晶区和回火区则存在一个软化区。通过组织分析, 对焊接热影响区的组织状态对焊接接头力学性能的影响进行了讨论。

关键词: 管线钢; 硬化; 软化; 高匹配
中图分类号: TG113 文献标识码: A 文章编号: 0253-360X(2005)09-19-05

0 序 言

迄今为止, X80管线钢是已建管线中强度最高的管线钢, 工业发达国家普遍将其列为 21世纪天然气输送管道的首选用钢。国内的 X80管线钢正在研制和开发阶段, 并已正式列入 "十·五"国家重大技术装备研制和国产化项目, 现已由武汉钢铁公司完成小批量的工业试制。

X80管线钢属超低碳、超细晶粒高强度合金钢, 在低碳及低硫的基础上, 以 Mn-Nb-Ti系为主, 适量添加 Ni、Mo、Cu等, 并结合控轧控冷(TMCP)等形变热处理技术, 从而控制奥氏体的再结晶温度, 阻止高温奥氏体的长大, 增加铁素体的形核核心以达到细化晶粒和微合金化元素析出相强化基体, 从而获得组织细小而强度和韧性很高的管线钢的目的[1]。X80管线钢组织主要成分为针状铁素体和粒状贝氏体, 其开发重点在提高材料的韧性方面, 即按控制裂纹扩展速度和扩展中止特性的合金化设计方案, 进行控轧工艺的最佳配合, 其合金元素的选择、终轧温度、冷却速度和终冷温度是生产工艺的控制关键。

根据美国标准 API 5L-1977, X80管线钢力学性能要求[1]为, 屈服强度 $\sigma_s \geqslant 551$ MPa, 抗拉强度 σ_b 620~827 MPa, 伸长率 $\delta_5 \geqslant 18\%$, 冲击吸收功 $A_{kV} \geqslant 68$ J(0℃)。其焊接性所要讨论的两个重要方面为裂纹敏感性和焊接热影响区的力学性能。对 X80管线钢组织和焊接性能特点进行研究分析, 为 X80管线钢用焊接材料的研制开发无疑具有重要的工程实际意义。

1 试验材料与方法

试验用钢板为武汉钢铁公司新研制的 X80管线钢, 厚度 15 mm, 焊接材料采用 H08MnMo+SJ101, 焊丝规格 φ4.0 mm, 采用双面焊接, 不对称 X形坡口, 正面焊完后反面清根埋弧焊接。焊接工艺参数为焊接电流 450~480 A, 电弧电压 30~32 V, 热输入 2 kJ/mm。钢板的化学成分见表 1。

表 1 X80管线钢的化学成分(质量分数, %)
Table 1 Chemical composition of X80 pipeline steel

C	Si	Mn	Nb	V	Ti	B	Cu	Ni	Mo	S	P	C_{eq}^{*}	P_{cm}^{*}
0.06	0.24	1.57	0.04	0.01	0.013	0.0006	0.045	0.14	0.29	0.005	0.033	0.394	0.233

*: $C_{eq}=C+Mn/6+(Cu+Ni)/15+(Cr+Mo+V)/15$[2]; $P_{cm}=C+Si/30+Mn/20+Cu/20+Ni/60+Cr/20+Mo/15+V/10+5B$[2]。

在焊接接头处分别截取母材、HAZ、焊缝区试样, 经过磨制、抛光处理和清洗后, 在 HV-120型维氏硬度计上做硬度测试(5 kg荷重)。在 JB-30B冲击试验机上进行冲击韧度试验, 拉伸试验在 PCS-25T试验机上进行, 并进行金相显微分析和扫描电镜断口形貌分析。

收稿日期: 2004-10-28
基金项目: 陕西省教育厅自然科学基金资助项目(01JK134)

2 试验结果及分析

2.1 热影响区硬度

碳当量 C_{eq}或标志晶内硬脆程度的最高硬度 H_{max}是评定焊接接头的淬透性和形成裂纹危险性的一个重要指标。从HAZ抗冷裂纹的能力来说，由于X80管线钢的碳当量的显著降低，HAZ淬硬成马氏体的可能性极小，冷裂纹敏感指数也明显减小，从而冷裂倾向小。

国际焊接学会（IIW）提出的焊接热影响区最大硬度试验的目的，是在一定的热循环下评定不同钢材焊接热影响区淬硬和冷裂倾向的大小。按国标GB 4675.5－84《焊接热影响区最高硬度试验方法》规定，垂直切断焊缝，抛光后进行硬度测试。图1是HAZ硬度分布特征曲线。

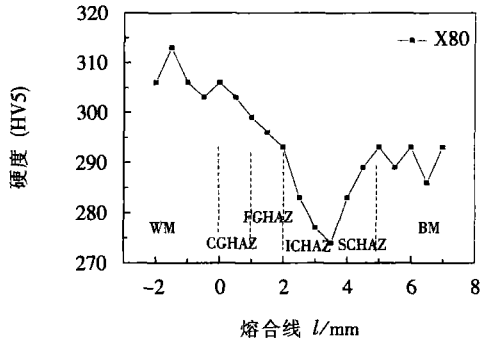

图1 HAZ硬度分布

Fig. 1 Distribution of hardness in HAZ

一般来说，低合金高强钢焊接接头的焊缝区、热影响区及母材三个区域中，HAZ是最薄弱环节。基于HAZ的组织特征，HAZ可再分为四个区[3]。

粗晶区（CGHAZ）——即熔合区和过热区，焊接热循环温度 $T_{max} \geqslant 1\,150$ ℃。

细晶区（FGHAZ）——即重结晶区，峰值温度超过 A_{c_3}（1 150 ℃$> T_{max} \geqslant$ 900 ℃）。

临界温度热影响区（ICHAZ）——即不完全重结晶区，峰值温度 $A_{c_3} \sim A_{c_1}$（900 ℃$> T_{max} \geqslant$ 700 ℃）。

亚临界温度热影响区（SCHAZ）——回火区，峰值温度在 A_{c_1} 以下（700 ℃$> T_{max} \geqslant$ 600 ℃）。

在显微镜下测定其组织分布状态，CGHAZ约1.5 mm，FGHAZ约1.0 mm，ICHAZ和SCHAZ约2.5 mm，热影响区的总长度为5.0 mm左右。

图1中的硬度测试结果表明，热影响区的最高硬度出现在CGHAZ，其值为305 HV低于美国标准API 5LS－1977的最高硬度＜350 HV[4]标准要求。焊接试样放置数周时效后切成试片，在光学显微镜下观察，热影响区、母材以及焊缝均无任何裂纹出现。然而，有研究[5]认为，在H_2S环境中使用的X80管线钢，HAZ最大允许硬度为248HV，显然，这次试验的X80管线钢超过了这一要求的限制范围。

图1的测试结果还表明，热影响区的最低硬度出现在ICHAZ和SCHAZ之间，即焊接接头存在有HAZ软化区。

2.2 焊接接头拉伸试验

焊接接头拉伸试验按国标GB 2651－81《焊接接头拉伸试验法》和国标GB 228－76《金属拉力试验法》进行，试验结果示于表2。

表2 X80管线钢拉伸试验结果

Table 2 Tensile test results of for X80 pipeline steel

	抗拉强度 σ_b MPa	屈服强度 σ_s MPa	伸长率 δ(%)	断面收缩率 ψ(%)	断口位置
母材	739～758	555～597	32～33	67～70	－
焊接接头	666～682	464～492	27～28	72～74	焊缝区

由表2可知，焊接接头的断口位置位于焊缝区，这表明焊接热影响区的强度高于焊缝，软化区的强度没有受到明显的影响。母材的拉伸曲线呈现为连续屈服现象，无明显的屈服平台，这是因为X80管线钢的针状铁素体基体是具有高密度的可移动位错，易于实现多滑移。

2.3 冲击试验

根据国标GB 2650－81《焊接接头冲击试验法》的相应规定进行焊接接头V形缺口冲击试验，试样尺寸10 mm×10 mm×55 mm，取样部位如图2所示。

图2中位置Ⅰ为熔合线，位置Ⅱ为距熔合线4 mm处。试验结果列于表3。

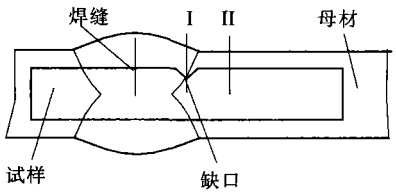

图 2　焊接接头冲击试验取样部位示意图

Fig. 2　Position of impact test samples from welded joint

表 3　X80管线钢焊接接头冲击试验结果(A_{kV}/J)

Table 3　Results of impact test for X80 pipeline steel

母材	焊缝	位置Ⅰ	位置Ⅱ
>367.5	221	318	>367.5

从冲击试验结果来看,熔合区的冲击吸收功降低,其原因和低强匹配的焊缝有关。热影响区的回火区冲击吸收功与母材相比并无明显差距。

2.4　焊接接头金相组织和断口形貌

焊接接头热影响区的金相组织见图 3。由于X80管线钢中的 Ti、Nb和 Mo等微合金元素形成微小的碳化物或氮化物粒子,从而会限制奥氏体晶粒的长大[6],单道焊时粗晶区晶粒不会太粗,但由于采用多层焊缝,后焊焊道的 HAZ与先焊焊道重叠,在先焊焊道的 HAZ中粗晶区经历后焊焊道的热输入(A_{c_1} ~A_{c_3}),因而导致 HAZ粗晶区组织再次粗化,从而形成在熔合区和过热区的临界温度间再热粗晶热影响区(ICCGHAZ)[3],最终得到了粗大的先共析铁素体,呈条状和块状(见图 3a、b)。

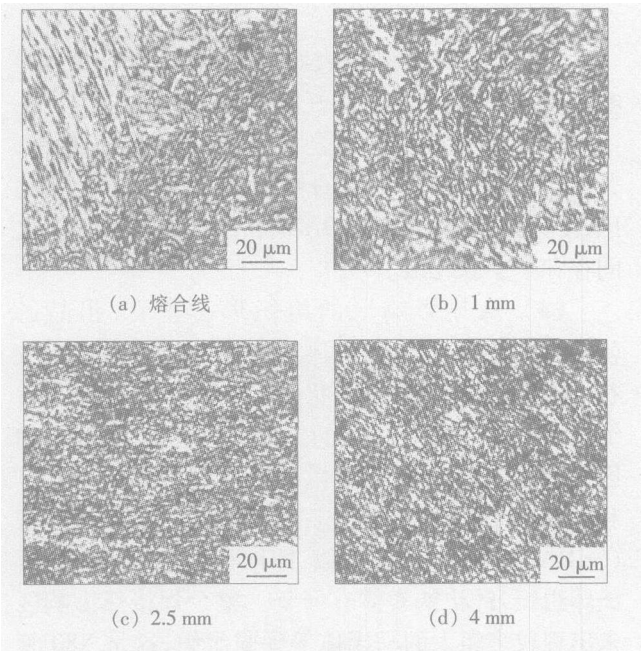

图 3　焊接接头金相组织距熔合线距离

Fig. 3　Optical metallograph of welded joint

当峰值温度在 1 150 ℃ ~A_{c_3}之间时,母材被加热至奥氏体化温度而快速冷却,所得到的组织为细小的铁素体组织,形成重结晶区(见图 3c)。在回火区内,峰值温度未超过 A_{c_1},因此其组织与母材相似,仍然保留原有组织的带状特征(见图 3d)。图 4为不完全重结晶区和母材金相组织图。

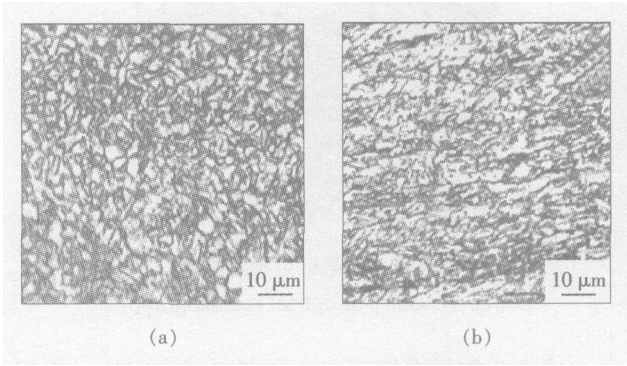

图 4　不完全重结晶区和母材金相组织

Fig. 4　Optical metallograph of ICHAZ and parent material

当峰值温度在 A_{c_3} ~A_{c_1}之间时,母材只发生部分重结晶,所得到的组织为细小的铁素体和由于受热晶粒影响稍有长大的针状铁素体,形成不完全重结晶区(ICHAZ)。由于多层焊,先焊焊道的 ICHAZ受到后焊焊道热输入(温度低于 A_{c_1})的影响,从而使组织回火回复,冷却后最后得到未发生相变的较粗大的铁素体和粗晶针状铁素体(CAF)[7]　和粒状贝氏体混合组织(见图 4a),这一结果表现为该处发生了软化现象。

焊接接头的力学性能与其组织是密切相关的。CGHAZ韧性降低与粗大的先共析铁素体和硬脆相岛状 M-A组元析出有关[7]。图 5为粗晶区金相组织,白色基体为粗大的先共析铁素体,小黑点为碳化物,而大块带棱角的黑色相为 M-A组元。M-A组元自身韧性较低,在粗晶铁素体基体周围产生应力集中[5],当 M-A组元的体积百分比较大时,就会形成局部脆性区(LBZ)[3,8]。由图 5可见,X80管线钢的 M-A组元含量并不高,这是因为 X80管线钢含碳量很低,而 M-A组元随碳含量而变化,研究认为[7],对于超低碳 TMCP钢(包括 X80管线钢)HAZ粗晶区,即使高热输入和缓冷条件,M-A组元产生都很少,这也是其粗晶区仍具有较高的冲击韧度的原因(见表 3)。

ICHAZ和 SCHAZ之间,即峰值温度在 900 ℃>T_{max}>600 ℃,出现了一个 HAZ软化区带。比较图 3d和图 4a、b可知,软化区较母材组织明显长大,可能是因为多层焊的热输入(温度低于 A_{c_1}),使得

这一区间的针状铁素体发生回复和再结晶而发生晶粒长大现象,结果表现为以位错结构形式储存的能量得以释放,位错密度下降,从而导致该区间出现了软化现象,即 HAZ的软化区问题。

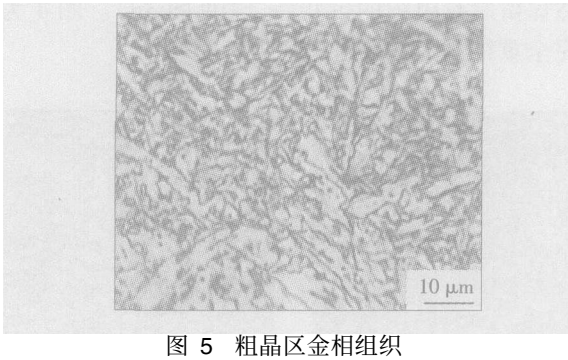

图 5 粗晶区金相组织

Fig. 5 CGHAZ opticalmetallograph

图 6为扫描电镜观察到的断口显微组织。将粗晶熔合区处断口 (见图 6a)与母材 (见图 6b)比较可见,母材回火区断口韧窝数量多,深度大,故表现出较好的塑性和韧性,断裂时冲击吸收功较大。粗晶熔合区断口中主要是由较小韧窝集聚而成的较大尺寸韧窝,韧窝深度较浅,数目变多,断裂时冲击吸收功低于母材。

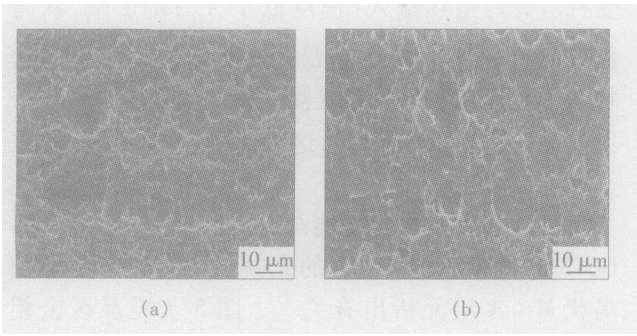

图 6 粗晶区和回火区冲击断口

Fig. 6 Fracture appearance at CGHAZ and SCHAZ

3 焊接性能与焊缝金属的高匹配

CGHAZ硬化脆化与 ICHAZ和 SCHAZ间的软化是焊接接头的薄弱环节。由于脆化区域靠近熔合线,形状复杂,宽度狭窄,超低碳钢改善了粗晶韧性,经验证明[8,9],粗晶脆化区对结构整体性的影响很小,而软化区更有可能促成裂纹的发展进而造成焊接接头失效。

软化对接头整体强度的影响受软化区的宽度、板厚和焊缝强度匹配等因素控制,这是因为当对 HAZ外加应力时,在软化区首先发生屈服,而随后的塑性变形受到相邻屈服应力较高的区域的约束,产生三轴应力,促使 Mises等效应力升高。研究认为[10],当软化区宽度与母材厚度之比小于 0.2时,软化区无明显塑性变形。然而,当软化区的相对宽度超过某一临界值 (超过板厚)时,接头相对抗拉强度会骤然下降,采用高匹配可提高软化区临界值[10]。图 7[11]为高、低匹配焊缝对母材以及焊接接头 HAZ性能的影响规律。

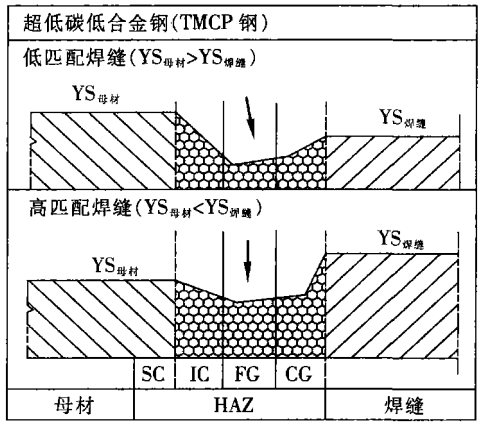

图 7 裂纹扩展路径预测

Fig. 7 Predicted crack propagation paths

焊缝采用更高的强韧性匹配时缺陷容限大于低匹配,可明显提高 TMCP低碳低合金高强钢 HAZ的强韧性[11],据此,X80管线钢焊缝金属宜采用高匹配。

4 结 论

(1) 焊接试验结果表明,X80管线钢焊接热影响区冷裂倾向小,具有良好的焊接性能。

(2) 硬度测试试验表明,X80管线钢焊接接头,其熔合区和过热区组成的粗晶区 (CGHAZ)为硬化区,不完全重结晶区 (ICHAZ)和回火区 (ICHAZ)之间存在一个软化区。

(3) 从热影响区的组织形态来看,粗晶区 (CGHAZ)组织为粗大的侧板条先共析铁素体和粒状贝氏体,并伴有少量岛状硬脆相 M-A组元析出;细晶区 (FGHAZ)为细小的铁素体;临界温度热影响区 (ICHAZ)为细小铁素体、粗晶针状铁素体 (CAF)和粒状贝氏体混合组织;亚临界温度热影响区 (SCHAZ)与母材组织类似,即针状铁素体加粒状贝氏体组织,针状铁素体有回复。整个焊接热影响区未出现较多粗大的马氏体等硬脆组织,这是 X80管线钢具有较好焊接性能的主要原因。

[下转第 26页]

$$Gap=\frac{\sum(GapEdgeR[i]-GapEdgeR[i])}{n},\quad(4)$$

式中：n是搜索出的边缘点的行数。

焊枪相对于摄像头是固定的，事先可以确定焊枪在图像中位置 TorchPosition。然后根据根部间隙中心线，计算出焊枪偏移量。

整个图像处理算法用时小于 200 ms。

5 结 论

（1）利用普通 CCD摄像机，附加窄带复合滤光片，拍摄到了清晰的根部间隙图像。

（2）根据对图像的分析，设计了首先利用缩小尺度法找到根部间隙的大概中心，然后再利用增强处理，找出根部间隙边缘的图像处理算法。

（3）该算法有效地提取出了根部间隙边缘，计算出根部间隙大小和焊枪相对于根部间隙的偏移量，为下一步利用普通 CCD摄像机实现 GMAW 焊缝跟踪奠定了基础。

参考文献：

[1] Liu Xinfeng, Gao Jingqiang, Jiang Xiresi, *et al*. Low cost automatic detecting of weld pool image in constant current TIG welding [J]. Transactions of the China Welding Institution, 2001, 22(6): 25-28.
刘新峰，高进强，姜锡瑞，等. 连续电流 TIG焊熔池图像的低成本自动化检测[J]. 焊接学报，2001，22(6)：25-28.

[2] Kovacevic R, Zhang Y M, Li L. Monitoring of weld joint penetration based on weld pool geometrical appearance [J]. Welding Journal, 1996, 75(10): 317s-329s.

[3] Pietrzak K A, Packer S M. Vision-based weld pool width control [J]. Transactions of the ASME, 1994, 116(1): 86-92.

[4] Kuo Hsing-Chia, Wu Li-Jen. An image tracking system for welded seams using fuzzy logic[J]. Journal of Materials Processing Technology, 2002, 120(1-3): 169-185.

[5] Chen Nian, Sun Zhenguo, Chen Qiang. A visual sensor based weld seam tracking method for precision pulse TIG welding[J]. Transactions of the China Welding Institution, 2001, 22(4): 17-20.
陈 念，孙振国，陈 强. 基于视觉图像传感的精密脉冲 TIG焊焊缝跟踪[J]. 焊接学报，2001，22(4)：17-20.

[6] Bae K Y, Lee T H, Ahn K C. An optical sensing system for seam tracking and weld pool control in gas metal arc welding of steel pipe[J]. Journal of Materials Processing Technology, 2002, 120(1-3): 458-465.

作者简介：高进强，男，工学博士，副教授。研究方向为焊接过程智能控制，发表论文 20余篇。

Email：jqg@sdu.edu.cn

[上接第 22页]

（4）焊接热影响区存在硬化和软化问题。硬化是过热和由于多层焊时粗晶区再热，即前焊道的粗晶区受后续焊道的再次加热引起的。软化则是由于热输入引起针状铁素体基体位错能释放所造成的，从焊接工艺上需控制热输入，可减小软化区宽度，而焊缝金属匹配上，采用高匹配更有利。

参考文献：

[1] 孔君华，郭 斌，聂斌英，等. 高钢级管线钢 X80的研制与发展[J]. 材料导报，2004，18(4)：23-26.

[2] 王晓香. 管线钢焊接常用的几种碳当量公式[J]. 焊管，2004，27(2)：71-73.

[3] Mlomozik. Effect of the welding thermal cycles on the structured changes in the heat affected zone and on its properties in joints welded in low alloy steels[J]. Welding International, 2000, 14(11): 8-12.

[4] American Petroleum Institute. API specification for spiral-weld line pipe[M]. Washington D. C.: American Petroleum Institute Production Department, API Spec 5LS Ninth Edition, 1977.

[5] Omweg G M, Frankel G S, Bruce W A, *et al*. Effect of welding parameters and H_2S partial pressure on the susceptibility of welded HSLA steels to sulfide stress cracking[J]. Welding Journal, 2003, 82(6): 136-144.

[6] 习天辉，陈 晓，袁泽喜. 大线能量焊接用钢热影响区组织和性能的研究进展[J]. 特殊钢，2003，24(5)：1-5.

[7] Bonnevie E, Ferriere G, Ikhlef A, *et al*. Morphological aspects of martensite austenite constituents in intercritical and coarse grain heat affected zones of structural steels[J]. Materials Science and Engineering A, 2004, 385(1-2): 352-358.

[8] 许祖泽. 新型微合金钢的焊接[M]. 北京：机械工业出版社，2004.

[9] Yurioka N. TMCP钢及焊接[J]. 武钢技术，1998，36(10)：61-64.

[10] Zhu Liang, Chen Jianbong. Stnength and deformation in HAZ-softened welded joins[J]. Iransactions of the China Welding Institution, 2004, 25(2): 61-65.
朱 亮，陈剑虹. 热影响区软化焊接接头的强度及变形[J]. 焊接学报，2004，25(2)：61-65.

[11] Pisarski H G, Dolby R E. The significance of softened HAZs in high strength structural steels[J]. Welding in the World, 2003, 47(5): 32-39.

作者简介：张 敏，男，1967年 7月出生，副教授，博士研究生。主要从事焊接结构断裂强度及焊接工程结构方面的研究，发表论文 20余篇。

Email：zhmm@263.net

MAIN TOPICS, ABSTRACTS & KEY WORDS

Prediction of grain size in the HAZ of the ultrafine grain steel joint

ZHAO Hong-yun[1,2], WANG Guo-dong[1], LI Dong-qing[3], LIU Xiang-hua[1], DU Lin-xiu[1] (1. State Key Lab Rolling and Automation, Northeastern University, Shenyang 110004, China; 2. School of Materials Science and Engineering, Changchun University of Technology, Changchun 130012, China; 3. School of Material Science and Engineering, Harbin Institute of Technology, Harbin 150001, China). p1 - 4

Abstract: The welding temperature field of the ultrafine grain steel was computer simulated in this paper, and the thermal cycle curve was obtained. The grain size in HAZ was predicted based on the thermal cycle curve. The outcome of the prediction was in accordance with the outcome of the experiment. The heat affected zone (HAZ) is one of the main areas which affect the properties of welds. It is essential meaningful to complete the prediction of grain size by computer using proper methods and that can provide a new and important foundation for optimizing welding parameters and improving the quality of welds. The result showed that: (1) The width of the HAZ was about 6.5 mm; (2) The grain size in HAZ increased obviously and the largest was 180 μm; (3) The higher the cooling speed was, the more refined the grain was, but the refined extent was relatively limited, not obvious.

Key words: ultrafine grain steel; thermal cycle curve; HAZ; grain size

Research on friction stir welding technology of T2-H62

LIU Xiao-wen, MU Yao-zhao, YANG Ning-ning, YAN Jun-hui (Material Institute, Northwestern Polytechnical University, Xi'an 710072, China). p5 - 8

Abstract: Friction stir welding of T2-H62 was investigated in this paper. Many experiments were carried on the welding machine modified by ourselves. The material, shape and dimension of the nib had been optimized. The significance sequence of processing parameters of friction stir welding had been calculated by signal-noise (SN) ratio experiments. The mechanical performance of T2-H62 welded joints was tested through tensile experiments, hardness tests and bending tests.

Key words: T2-H62; friction stir welding; SN ratio experiment

Auxiliary transformer FB-ZVZCS PWM inverter arc welding power supply

FANG Chen-fu[1,2], YIN Shu-yan[1], HOU Run-shi[2], WEN Yong-ping[2], YU Ming[2], LI Jun[3] (1. College of Mechanical Engineering & Applied Electronics Technology, Beijing Polytechnic University, Beijing 100022, China; 2. School of Material Science and Engineering, Jiangsu University of Science and Technology, Jiangsu Zhenjiang 212003, China; 3. Kaierda Electric Welding Machine Co. Ltd., Hangzhou 310018, China). p9 - 12

Abstract: The decreasing time of freewheeling current is relative to duty cycle in the exiting FB-ZVZCS-PWM soft switching inverter arc welding power supply with the block capacitor, and it is hard to achieve zero current switching (ZCS) for lagging leg with low duty cycle. By adopting auxiliary transformer in the primary side of main transformer, the decreasing time of freewheeling current is independent of duty cycle, which is proportion to the peak current in the primary side of main transformer. A new FB-ZVZCS-PWM soft switching inverter arc welding power supply was introduced, which adopted the auxiliary transformer and limited bipolar control mode. The principles of realizing zero voltage switching (ZVS) for leading leg by capacitor and ZCS for lagging leg by auxiliary transformer were explained. Simulation and experimental results showed that the soft switching could be realized under all loads as long as the auxiliary transformer was designed by the maximum peak current in the primary side of main transformer.

Key words: soft switching; inverter; arc welding; power supply

Finite element analysis of friction stir welding process

ZHANG Hong-wu, ZHANG Zhao, CHEN Jin-tao (State Key Laboratory of Structural Analysis for Industrial Equipment, Dalian University of Technology, Liaoning Dalian 116024, China). p13 - 18

Abstract: Friction stir welding (FSW) is a new solid-state joining process which was invented by The Welding Institute in 1991. FSW has been found to be effective for joining hard-to-weld metals and for joining plates with different thickness or different materials. 2D numerical model was constituted in this paper and then the friction stir welding process was simulated. The parameters of FSW process, the flow of the material and the stress and strain in the FSW process were studied. Compared with the data of the experiments, numerical results were shown to demonstrate the efficiency and the validity of the model developed.

Key words: friction stir welding; residual stress; finite element simulation; welding process

Analysis of weldability of X80 pipeline steel

ZHANG Min[1], YAO Cheng-wu[1], NIE Bin-ying[2] (1. School of Material Science and Engineer

ing, Xi'an University of Technology, Xi'an 710048, China; 2. Yichun University, Jiangxi Yichun 336000, China). p19 - 22, 26

Abstract: The mechanical properties and weldabilities of X80 pipeline steel were investigated by testing hardness, tensile strength and impact toughness in this paper. The result showed that the toughness of CGHAZ decreased because of the hardening and embrittling substance appeared in coarse-grained heat affected zone (CGHAZ), and there was a softening zone between the intercritical heat affected zone (ICHAZ) and the subcritical heat affected zone (SCHAZ). The effect of the organization on X80 mechanical properties was discussed also.

Key words: pipeline steel; hardening; softening; overmatching

Vision based detection of root gap and deviation between torch and gap centerline in GMAW GAO Jin-qiang[1,2,3], WU Chuan-song[1], LIU Xi-zhang[2], XIA Dian-xiu[2] (1. Key Laboratory of Structure and Heredity of Materials, MOE, Shandong University, Jinan 250061, China; 2. Post-doctorate Work Station, Jinan Iron & Steel Group Corp., Jinan 250101, China; 3. Post-doctorate Mobile Stations, Tianjin University, Tianjin 300072, China). p23 - 26

Abstract: Weld seam tracking is an important aspect of welding quality control and GMAW (gas metal arc welding) is widely used in industries. An image of root gap in GMAW was captured using CCD camera and composite filter lens. An algorithm was designed based on the analysis of gray characteristics of the root gap. Root gap edges could be extracted by the algorithm. Thus the gap and the deviation between torch and root gap centerline could be obtained. This work has laid a solid foundation to realize the GMAW weld seam tracking.

Key words: weld seam tracking; root gap; GMAW; image

Impact properties of 6063 Al alloy FSW weld CHAI Peng, JIAN Bo, JI Ya-juan, LUAN Guo-hong (China FSW Center, Beijing Aeronautical Manufacturing Technology Research Institute, Beijing 100024, China). p27 - 30

Abstract: Aluminum extrusions were widely used in rolling stock, automobile and aerospace, et al. In this paper, based on friction stir welding (FSW) technology and equipment for aluminum extrusions, impact properties, plastic deformation capacity and microstructure of 6063-T651 FSW weld were studied. The results showed that there were fine dynamic recrystallized grain in FSW weld, precipitation was dispersedly distributed, and impact properties and plastic deformation capacity of the weld was approximately the same with that of the base material.

Key words: 6063 aluminum extrusion; friction stir welding; impact toughness

Reliability test and analysis of 1.27 mm pitch plastic ball grid array soldered joint under thermal shock HUANG Chun-yue[1,2], WU Zhao-hua[2], ZHOU De-jian[2] (1. School of Electro-Mechanical Engineering, Xidian University, Xi'an 710071, China; 2. Department of Electronic Machinery and Transportation Engineering, Guilin University of Electronic Technology, Guangxi Guilin 541004, China). p31 - 34

Abstract: The soldered joint reliability of 1.27mm pitch plastic ball grid array (PBGA) package was studied by Taguchi design experiment method under the thermal shock. The stencil thickness, the pad diameter and the chip weight were chosen as the three critical factors for the design of the PBGA test specimens by using a Taguchi orthogonal array. The thermal shock cycling test of PBGA test specimens was carried out. The range analysis and the variance analysis were performed to determine both the best combination of the process parameters and the most influential factors; the failure distribution of PBGA soldered joints was also characterized by using two-parameter Weibull distribution. The results show that the thickness of stencil has a significant effect on the reliability of the 1.27mm pitch PBGA soldered joints. The optimal of process parameters are the stencil thickness of 0.15mm, the pad diameter of 0.73mm and the chip weight of 18.0547g. The failure life of PBGA soldered joint follows the two-parameter Weibull distribution, whose shape parameter and scale parameter are 0.85 and 6254.88, respectively.

Key words: design of experiment; plastic ball grid array; process parameters; range analysis; variance analysis

The numerical simulation of the brazing process of cemented carbide cirque and steel YUE Xi-shan, SUN Feng-lian (College of Material Science and Engineering, Harbin University of Science and Technology, Harbin 150040, China). p35 - 38, 43

Abstract: Aiming at brazing crack induced by thermal stress during the process of brazing, finite element method was used to analyze the residual stress of joints between the cemented carbide cirque and steel. The effects of joint shapes and filler metal thickness on the distribution of residual stress were researched. The result showed that notch was disadvantageous to the strength of joints, and the optimal value of filler metal thickness existed. The calculated result was consistent with that of the experiment.

Key words: cemented carbide cirque; brazing; residual stress; numerical simulation

Safe assessment of surface flaw under mismatched weld in offshore pipeline XIA Jing[1], HUO Li-xing[1], BAI Bing-ren[2], CAO Jun[2] (1. School of Materials Science and Engineering, Tianjin University, Tianjin 300072, China; 2. China Offshore Oil Engineering Limited Company,